Supporting Information

Sol-Gel Synthesis of Spherical Mesoporous High-Entropy-Oxides

Gen Wang, [†‡‖] *Jing Qin*, [†‖] *Youyou Feng*, [†] *Bingxi Feng*, [†] *Shengjiong Yang*, [‡] *Zheng Wang*, [§] *Yongxi Zhao*, [†] *and Jing Wei* [†*]

[†]Institute of Analytical Chemistry and Instrument for Life Science, The Key Laboratory of Biomedical Information Engineering of Ministry of Education, School of Life Science and Technology, Xi'an Jiaotong University, Xi'an, Shaanxi, 710049, P. R. China.

[‡]Shannxi Key Laboratory of Environmental Engineering, School of Environmental and Municipal Engineering, Xi'an University of Architecture and Technology, Xi'an, Shaanxi 710055, P. R. China.

[§]State Key Laboratory of High-efficiency Utilization of Coal and Green Chemical Engineering, College of Chemistry and Chemical Engineering, Ningxia University, Ningxia, 750021, P. R. China.

Corresponding Author

E-mail: jingwei@xjtu.edu.cn (J.W.).

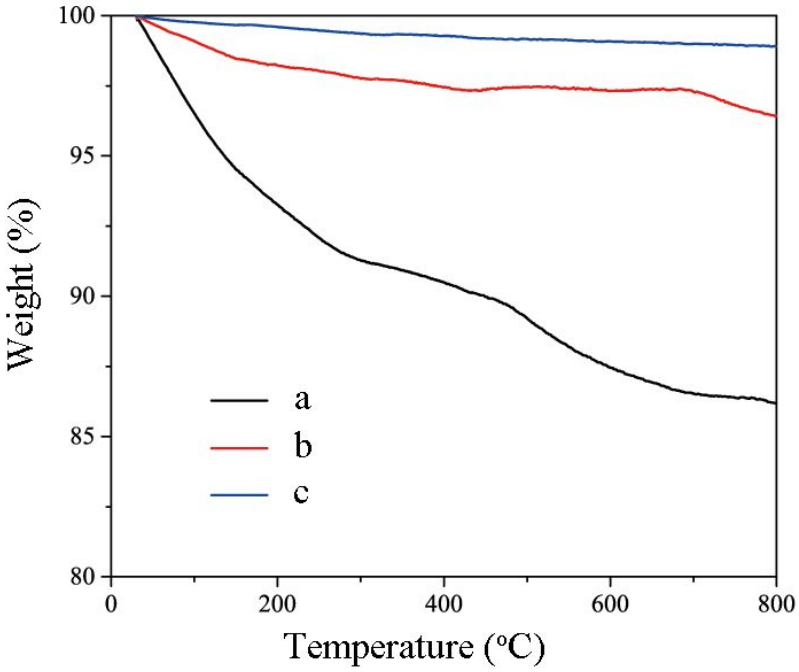

Figure S1 TG curves for (a) Ni-Co-Cr-Fe-Mn-TF-400, (b) Ni-Co-Cr-Fe-Mn-TF-600 and (c) Ni-Co-Cr-Fe-Mn-TF-900 in air. The ramp rate: 10 ºC/min.

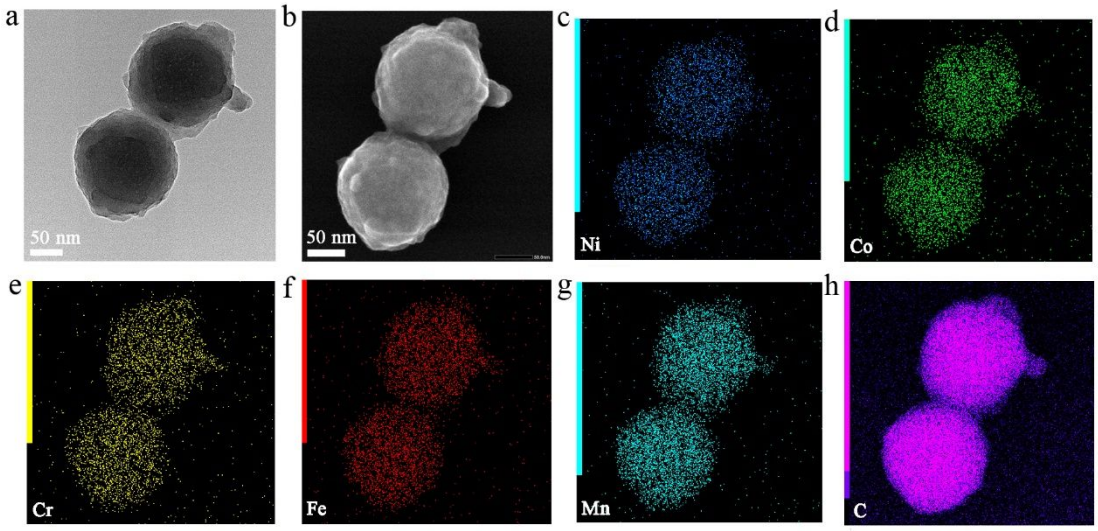

Figure S2 (a) TEM, (b) STEM, and (c-h) element mapping images for Ni-Co-Cr-Fe-Mn-TF polymer spheres.

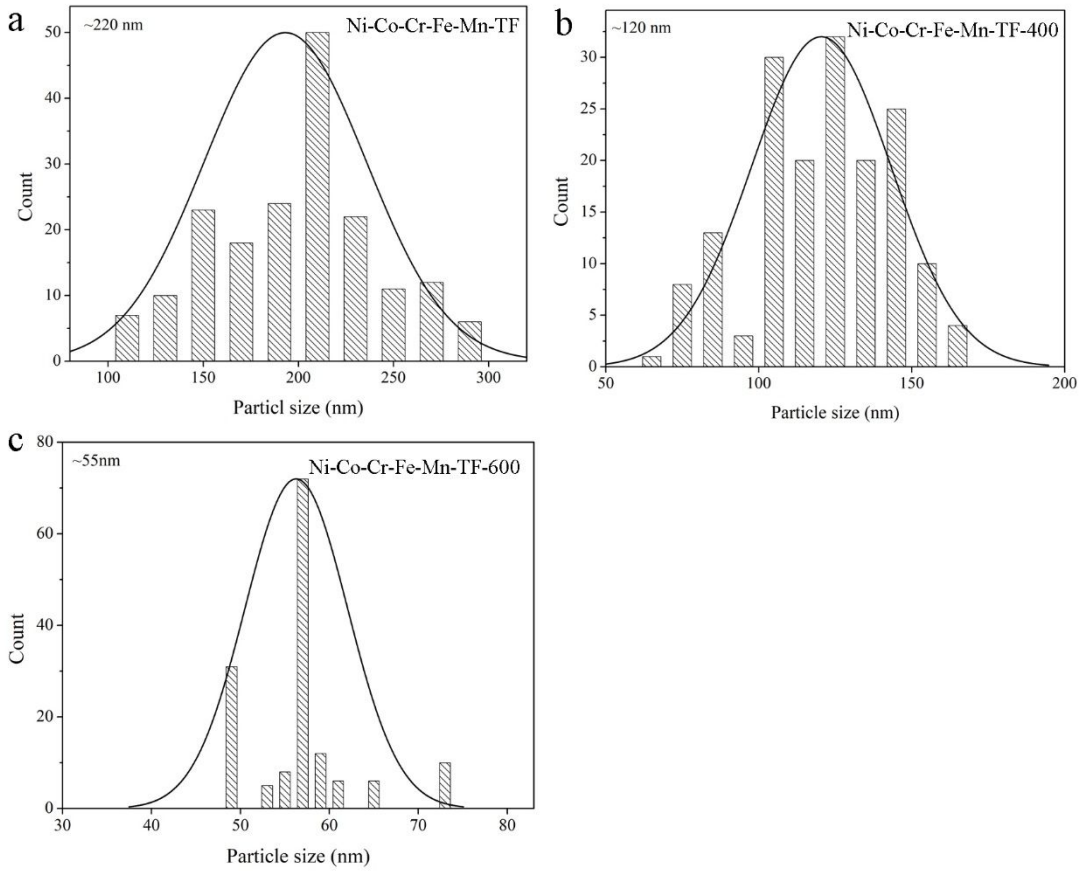

Figure S3 The particle size distributions for (a) Ni-Co-Cr-Fe-Mn-TF, (b) Ni-Co-Cr-Fe-Mn-TF-400 and (c) Ni-Co-Cr-Fe-Mn-TF-600 calculated from TEM results.

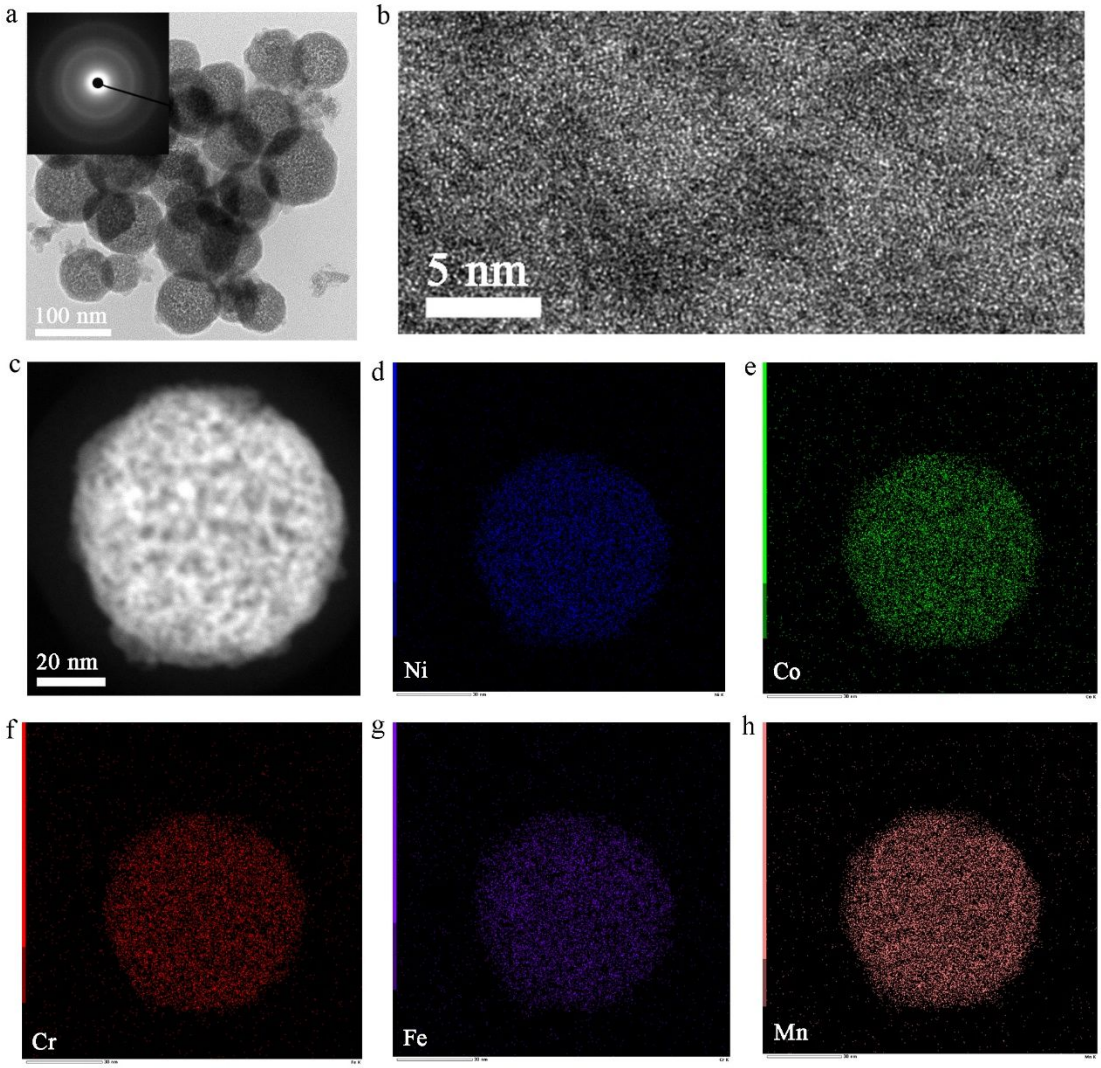

Figure S4 (a-b) TEM, (c) STEM and (d-h) corresponding element mapping images for Ni-Co-Cr-Fe-Mn-TF-400 obtained by calcination at 400 ºC. Inset in (a) was the SAED patterns.

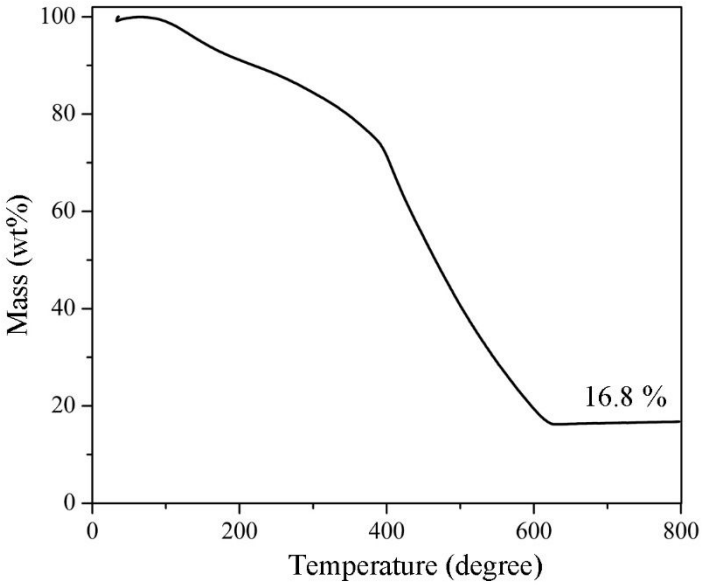

Figure S5 TG curves for Ni-Co-Cr-Fe-Mn-TF measured in air.

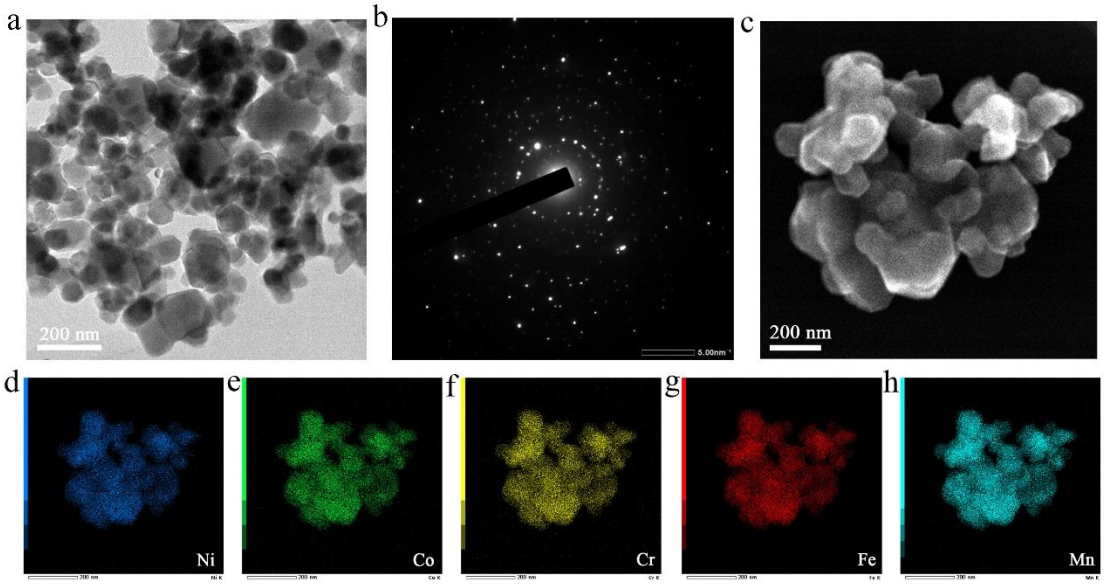

Figure S6 (a) TEM image, (b) SAED patterns, (c) STEM image and (d-h) corresponding element mapping for Ni-Co-Cr-Fe-Mn-TF-900: (d) Ni, (e) Co, (f) Cr, (g) Fe, (h) Mn.

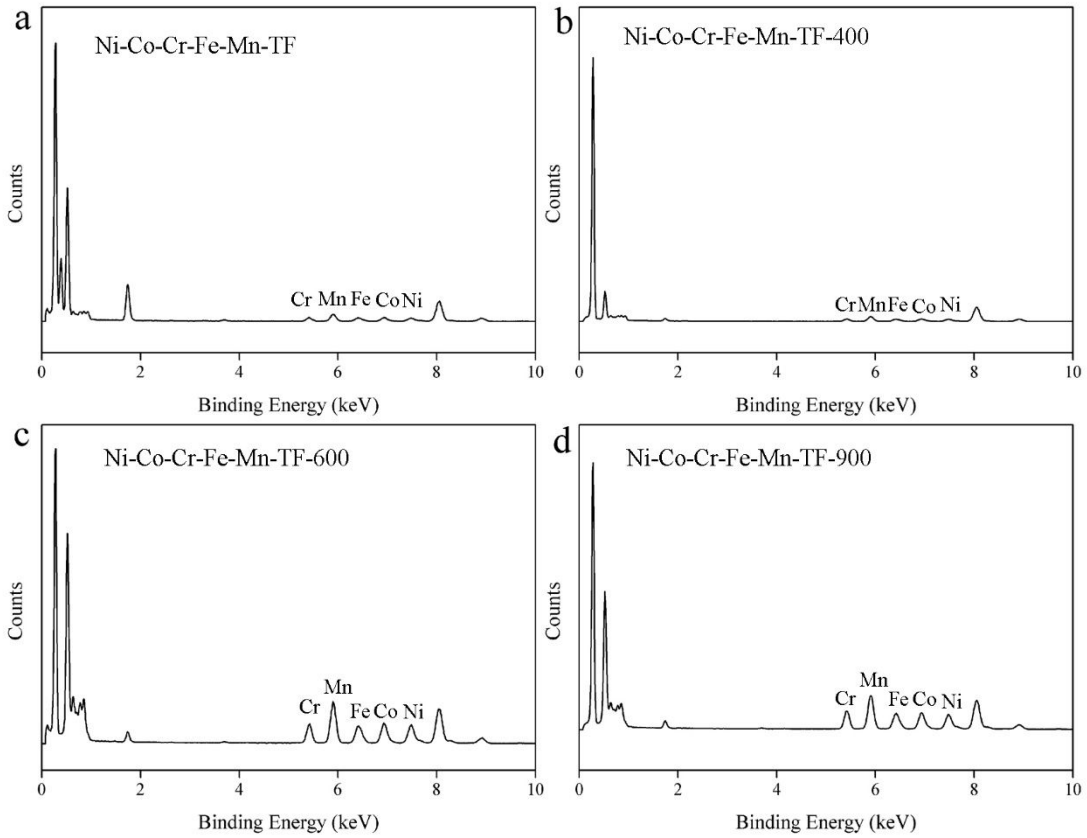

Figure S7 Energy dispersive X-ray spectroscopy (EDX) for (a) Ni-Co-Cr-Fe-Mn-TF, (b) Ni-Co-Cr-Fe-Mn-TF-400, (c) Ni-Co-Cr-Fe-Mn-TF-600 and (d) Ni-Co-Cr-Fe-Mn-TF-900.

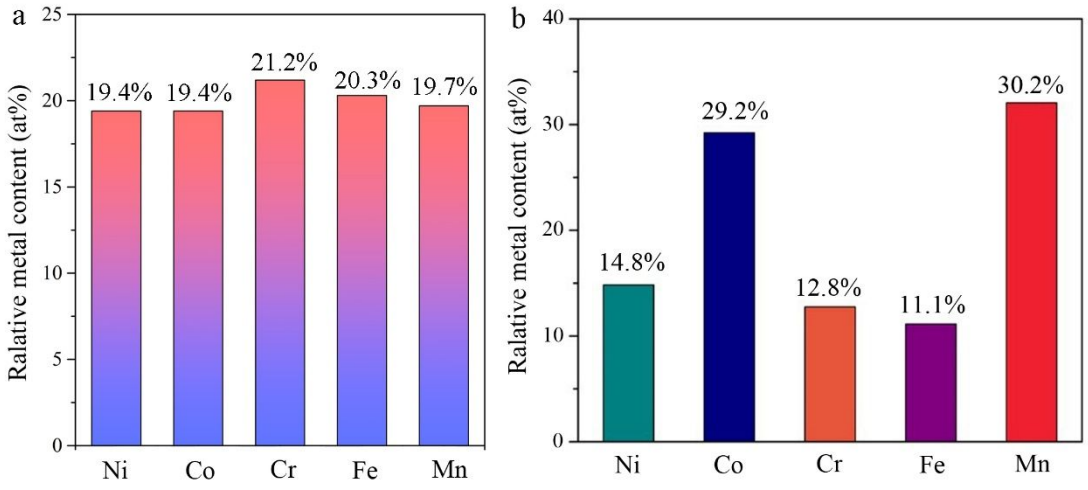

Figure S8 Relative metal contents in (a) metal precursor and (b) mesoporous HEOs (Ni-Co-Cr-Fe-Mn-TF-600).

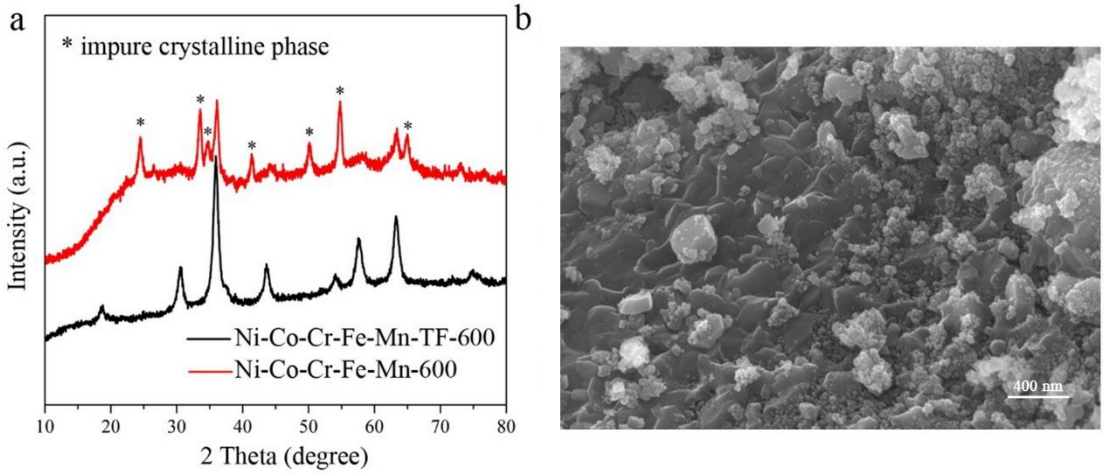

Figure S9 (a) XRD patterns and (b) SEM image for Ni-Co-Cr-Fe-Mn-600. The metal oxides (Ni-Co-Cr-Fe-Mn-600) were prepared by hydrolyzation of five different kinds of metal sources in the alkaline conditions without using TA as an organic ligand. The other synthesis procedures were like that of Ni-Co-Cr-Fe-Mn-TF-600. XRD results for Ni-Co-Cr-Fe-Mn-600 suggested the existence of impure phase. SEM image showed that Ni-Co-Cr-Fe-Mn-600 had an irregular morphology.

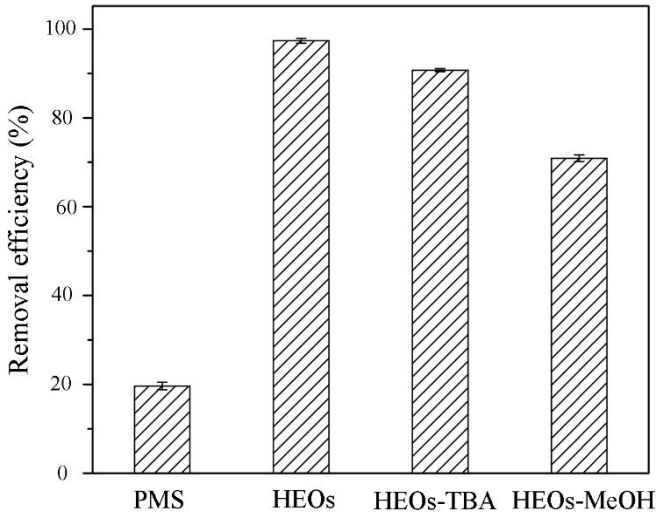

Figure S10 Effect of quenching agents on HEOs/PMS oxidation ($[MB]_0$ = 5 mg/L, $[PMS]_0$ = 0.45 μM, [HEOs] = 0.02 g/L, T = 25 ^oC).

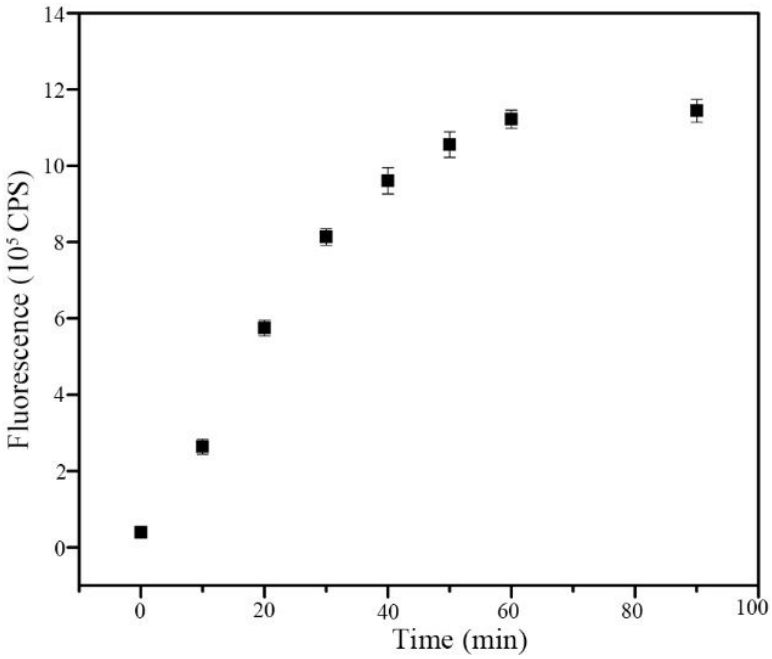

Figure S11 Fluorescence intensities versus different time after adding target DNA.

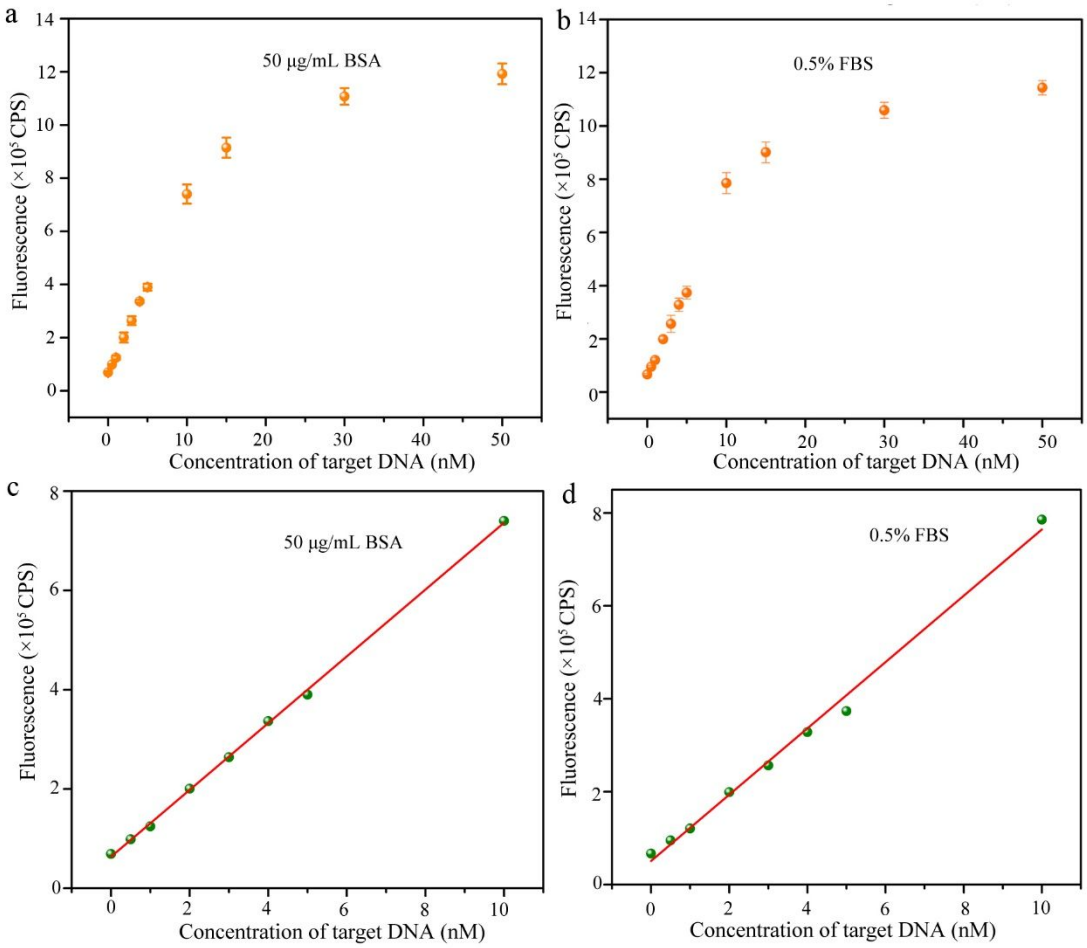

Figure S12 Fluorescence intensities versus different concentrations of target DNA (0.5-50 nM) in 50 μg/mL of BSA (a) and 0.5% FBS (b). The corresponding calibration curve for target DNA detection in 50 μg/mL of BSA (c) and 0.5% FBS (d).

Table S1 Textural properties for the reported HEOs.

Materials	BET surface area (m^2/g)	Pore size (nm)	Particle size (nm)	Application	Reference
$PtNiMgCuZnCoO_x$	28	N.A.	N.A.	catalytic oxidation of CO	1
$(CuNiFeCo)O_x$-Al_2O_3	129	3.9	N.A.	catalytic oxidation of CO	2
$(CuNiFeCoMg)O_x$-Al_2O_3	198	4.8	N.A.	catalytic oxidation of CO	2
$Co_{0.2}Ni_{0.2}Cu_{0.2}Mg_{0.2}Zn_{0.2}O$	42	N.A.	N.A.	aerobic oxidation of benzyl alcohol	3

Table S2 Textural properties for mesoporous HEOs.

Materials	BET surface area (m^2/g)	Pore volume (cm^3/g)	Pore size (nm)	Particle size (nm)
Ni-Co-Cr-Fe-Mn-TF polymer	5.4	0.02	5.7	220
Ni-Co-Cr-Fe-Mn-TF-400	143.4	0.38	8.3	120
Ni-Co-Cr-Fe-Mn-TF-600	72.2	0.36	7.8	22
Ni-Co-Cr-Fe-Mn-TF-900	41.9	0.18	5.5	N.A.

Table S3 The performance of different nanomaterials for DNA detection

Materials	Fluorescent reporter	Sensitivity (detection limit)	Detection time	Reference
GO	FAM	2 nM	5 min	4
GO	Silver nanoclusters	0.5 nM	1-1.5 h	5
MoS_2	FAM	0.5 nM	5 min	6
TiS_2	FAM Texas red	0.2 nM	5 min	7
Co_3O_4	FAM	0.19 nM	1 h	8
CoOOH	FAM	0.5 nM	5 min	9
Cu(H_2dtoa)	TFO	1.3 nM	3 h	10
Cu-TA crystals	FAM	0.74 nM	1 h	11
Spherical mesoporous HEOs	FAM	0.14 nM (Tris-HCl buffer)	1 h	***This work***
Spherical mesoporous HEOs	FAM	0.18 nM (bovine serum albumin)	1 h	***This work***
Spherical mesoporous HEOs	FAM	0.16 nM (fetal bovine serum)	1 h	***This work***

References

(1) Chen, H.; Fu, J.; Zhang, P.; Peng, H.; Abney, C. W.; Jie, K.; Liu, X.; Chi, M.; Dai, S. Entropy-Stabilized Metal Oxide Solid Solutions as CO Oxidation Catalysts with High-Temperature Stability, *J. Mater. Chem. A*, **2018**, *6*, 11129-11133.

(2) Zhang, Z.; Yang, S.; Hu, X.; Xu, H.; Peng, H.; Liu, M.; Thapaliya, B. P.; Jie, K.; Zhao, J.; Liu, J.; Chen, H.; Leng, Y.; Lu, X.; Fu, J.; Zhang, P.; Dai, S. Mechanochemical Nonhydrolytic Sol-Gel Strategy for the Production of Mesoporous Multimetallic Oxides, *Chem. Mater.* **2019**, *31*, 5529-5536.

(3) Feng, D.; Dong, Y.; Zhang, L.; Ge, X.; Zhang, W.; Dai, S.; Qiao, Z. Holey Lamellar High Entropy Oxide as Ultra-Highly Active Heterogeneous Catalyst for Solvent-free Aerobic Oxidation of Benzyl Alcohol. *Angew. Chem. Int. Ed*. **2020**, 10.1002/anie.202004892.

(4) Lu, C.; Yang, H.; Zhu, C.; Chen, X.; Chen, G. A Graphene Platform for Sensing Biomolecules. *Angew. Chem. Int. Ed*. **2009**, *48*, 4785-4787.

(5) Liu, X.; Wang, F.; Aizen, R.; Yehezkeli, O.; Willner, I. Graphene Oxide/Nucleic-Acid-Stabilized Silver Nanoclusters: Functional Hybrid Materials for Optical Aptamer Sensing and Multiplexed Analysis of Pathogenic DNAs. *J. Am. Chem. Soc*. **2013**, *135*, 11832-11839.

(6) Wang, Q.; Wang, W.; Lei, J.; Xu, N.; Gao, F.; Ju, H. Fluorescence Quenching of Carbon Nitride Nanosheet through Its Interaction with DNA for Versatile Fluorescence Sensing. *Anal. Chem.* **2013**, *85*, 12182-12188.

(7) Zhu, C.; Zeng, Z.; Li, H.; Li, F.; Fan, C.; Zhang, H. Single-Layer MoS_2-Based Nanoprobes for Homogeneous Detection of Biomolecules. *J. Am. Chem. Soc*. **2013**, *135*, 5998-6001.

(8) Wang, G.; Qin, J.; Zhou, X.; Deng, Y.; Wang, H.; Zhao, Y.; Wei, J. Self-Template Synthesis of Mesoporous Metal Oxide Spheres with Metal-Mediated Inner Architectures and Superior Sensing Performance. *Adv. Funct. Mater*. **2018**, *28*, 1806144.

(9) Chang, Y.; Zhang, Z.; Liu, H.; Wang, N.; Tang, J. Cobalt Oxyhydroxide Nanoflake

Based Fluorescence Sensing Platform for Label-Free Detection of DNA. *Analyst* **2016**, *141*, 4719.

(10) Zhu, X.; Zheng, H.; Wei, X.; Lin, Z.; Guo, L.; Qiu B.; Chen, G. Metal-Organic Framework (MOF): a Novel Sensing Platform for Biomolecules. *Chem. Commun.* **2013**, *49*, 1276-1278.

(11) Huang, H.; Qin, J.; Wang, G.; Guo, Z.; Yu, X.; Zhao, Y.; Wei, J. Synthesis of Spiny Metal-Phenolic Coordination Crystals as a Sensing Platform for Sequence-Specific Detection of Nucleic Acids. *CrystEngComm*, **2018**, *20*, 7626-7630.